The energy profile of polymorphous PbTe films. I. Direct energy gaps in PbTe high-pressure phases and energies of the heterophase junctions

1992 J. Phys.: Condens. Matter 4 8997

(http://iopscience.iop.org/0953-8984/4/46/007)

J. Phys.: Condens. Matter 4 (1992) 8997–9008. Printed in the UK

The energy profile of polymorphous PbTe films: I. Direct energy gaps in PbTe high-pressure phases and energies of the heterophase junctions

M Baleva, E Mateeva and M Momtchilova
Faculty of Physics, University of Sofia, 1126 Sofia, Bulgaria

Received 31 March 1992, in final form 23 June 1992

Abstract. The transmittance and reflectance spectra of polymorphous PbTe films grown by laser-assisted deposition on KCl substrates were investigated in the range between 400 and 4000 cm^{-1}. The refractive index dispersions $n(E)$ were obtained from the spectra. The energy gaps E_g of the high-pressure (HP) PbTe phases were determined from the maxima in the dependences $n(E) - E_g = 0.23$ eV for the BCC HP PbTe phase and $E_g = 0.42$ eV for the orthorhombic HP PbTe phase. The additional maxima in the $n(E)$ dependences were related to transitions across the heterophase junctions formed in the process of growth. The energy profiles of films grown under different technological conditions were obtained.

1. Introduction

PbTe belongs to the group of compounds with an average of five electrons per atom, which are well known to be highly unstable and easily undergo structural phase transitions even on a slight change in temperature and/or pressure. Pressure-induced phase transitions in the cubic A^4B^6 compounds and, in particular, PbTe have been studied by volumetric, electrical conductivity and x-ray diffraction methods (Chattopadhyay *et al* (1984) and references therein). PbTe has been reported to transform from the FCC NaCl-type structure to the orthorhombic GeS-type layered structure at pressures between 4.5 and 6 GPa (Wakabayashi *et al* 1968). A further structural phase transition to the BCC CsCl-type structure takes place at pressures of about 16 GPa (Chattopadhyay *et al* 1984, Fujii *et al* 1984). Electron microscopy and x-ray studies of PbTe films grown by laser-assisted deposition (LAD) showed the presence of the high-pressure (HP) CsCl- and GeS-type phases together with the ambient NaCl-type phase (Baleva 1986, Baleva *et al* 1992a, b). It was also found that the relative quantities of the three different crystal modifications depended on the technological conditions. Hence films with a prevailing content of one of the phases can be grown. A significant thickness of the sublayers containing the HP phases provided the possibility of studying the properties of these phases. From the study of the transmittance and reflectance, some preliminary results about the optical energy gap of the BCC PbTe phase have been obtained in our laboratory (Baleva 1986). In our recent studies we have obtained the frequencies of the IR-active modes in the HP phases as well as the Raman-active modes in the orthorhombic phase (Baleva *et al* 1992a, b). Apart from the determination of the existence of the HP phases

0953-8984/92/468997+12$07.50

and their crystal structure, study of their properties has barely been undertaken in bulk materials under hydrostatic pressure and that is why information about them is comparatively rare.

The purpose of the present work was to determine the optical energy gaps of the HP PbTe crystal phases from an investigation of the transmittance and reflectance spectra.

2. Sample characterization

Films of PbTe and PbTe doped with 0.2 and 0.3 mol% Cr were grown by LAD on (100)-oriented KCl substrates. The technological conditions which can be varied are the substrate temperature T_s, the laser energy per pulse and the substrate-to-target distance. The carrier concentration p and the Hall mobility μ were calculated from the Hall coefficient R_H and the electrical conductivity σ, measured by the standard Van der Pauw technique. The low values of μ at such carrier concentrations (table 1) indicate the presence of potential barriers in the samples. The film thicknesses were determined from pictures of the cross sections taken with an electron scanning microscope. The data on substrate temperatures, film thicknesses and kinetic parameters are given in table 1. In the labelling of the samples, K stands for a KCl substrate and T for PbTe; the notation CR means that the samples are doped with Cr and the number after the notation CR shows the amount of the dopant (e.g. CR3 means that the film is doped with 0.3 mol% Cr).

The investigation of the crystal structure has shown that all films with thicknesses greater than 1 μm represent a two-layer structure consisting of a relaxed FCC phase upper sublayer (which was formed in the final stage of growth) and a strained sublayer (which consists of HP phases). These investigations have also shown that the content of the HP phases in the strained sublayer is most sensitive to the substrate temperature T_s. At $T_s \leqslant 50$–100 °C, epitaxial growth of the (111)-oriented BCC phase takes place and the strained sublayer consists entirely of this phase, which is demonstrated in figure 1, sample CR2K10T. On increase in T_s the quantity of the orthorhombic phase increases and at a temperature T_s of about 250–300 °C it prevails to a great extent, as is seen in figure 1, sample CR2K3T. X-ray structural investigations show that the orthorhombic phase is polycrystalline. We have not succeeded in obtaining films with strained sublayers containing solely orthorhombic phase. This can be easily understood if one takes into consideration the volumetric investigations of Chattopadhyay *et al* (1984), according to which the structural phase transition from the orthorhombic to BCC phase is accompanied by large two-phase regions. In figure 2, representing the pressure-induced change in the volume of the various phases obtained by Chattopadhyay *et al* (1984), the regions of the BCC and the orthorhombic phase volume changes in our samples are shown by full and broken arrows, respectively. In the figure, V is the pressure-dependent volume of the PbTe lattice, calculated with the lattice constants obtained from the x-ray investigations, and V_0 is the volume at the pressure $p = 0$. It is seen that really the strained sublayer may consist either of BCC phase alone or of a mixture of HP phases, but never solely of orthorhombic phase. It is also worth noting that according to our x-ray investigations the CsCl- and GeS-type phases exist at a pressure as low as about 2.5 GPa. The finding is not surprising if one takes into account the experiments of Fujii *et al* (1984). They have shown that on reducing the pressure the BCC phase

Table 1. Substrate temperatures, thicknesses, carrier concentrations, Hall mobilities, activation energies and energy gaps of the samples. When two or three phases are given in the last column, it means that their quantities are comparable.

Sample	T_s (°C)	d (μm)	p, 300 K (cm^{-3})	μ, 300 K ($cm^2\,\Omega^{-1}\,°C^{-1}$)	$\Delta E = E_n^{FCC} - E_n^{orth}$ (eV)	E_g^{FCC} (eV)	E_g^{BCC} (eV)	E_g^{orth} (eV)	Prevailing crystal phases
K217T	150	5.6	7.5×10^{17}	980	—	0.32	—	—	FCC
K1010aT	280	4.5	5.4×10^{16}	190	0.06	0.32	—	—	FCC
K2411T	250	2.6	3.1×10^{17}	800	0.047	0.32	—	—	FCC
CR3K04T	300	1.1	—	—	—	0.32	Screened	0.42	FCC+orthorhombic
CR3K01T	50	1.1	—	—	—	Screened	0.23	—	FCC+BCC
K123T	95	0.9	—	—	—	Screened	Screened	0.42	FCC+orthorhombic+BCC
CR2K10T	50	0.7	—	—	—	0.32	0.23	—	BCC
CR2K3T	300	0.75	2.7×10^{17}	200	—	Screened	0.23	0.42	Orthorhombic

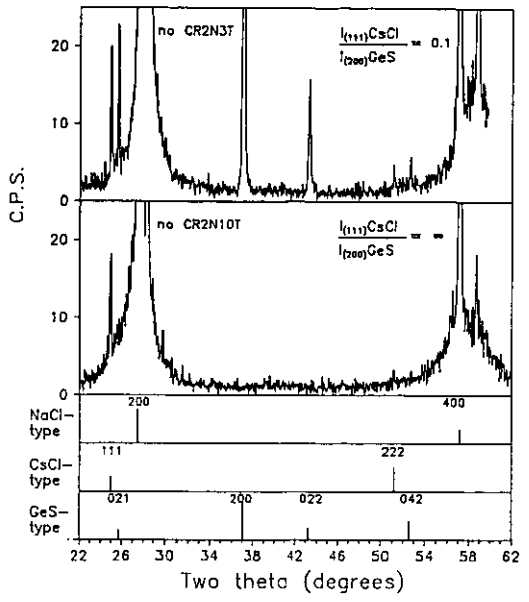

Figure 1. X-ray diffraction pattern of two samples, containing different quantities of the HP phases in their strained sublayers.

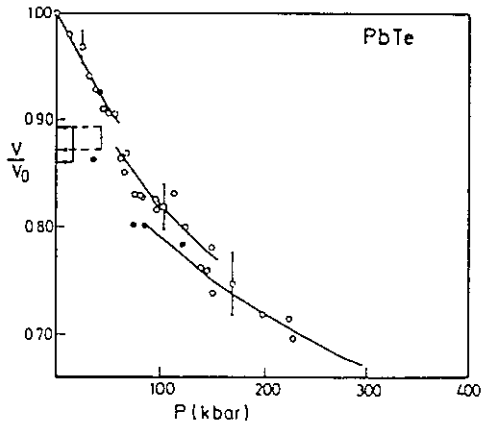

Figure 2. Pressure-dependent change in the volume of the different PbTe phases, obtained by Chattopadhyay *et al* (1984). The regions of BCC and orthorhombic phase volume changes in our samples are shown by full and broken arrows, respectively.

exists in the whole range between 16 GPa (the pressure of the phase transition) and 8 GPa, but they have not carried out experiments at pressures lower than 8 GPa.

The V/V_0 pressure dependence (figure 2) shows a sharp discontinuity in the transition from the orthorhombic to the FCC phase. The latter explains the presence of a well defined boundary between the strained (BCC or orthorhombic + BCC phases) and the relaxed (FCC phase) sublayers and, hence, the usually observed periodic modulation of the interference spectra of the comparatively thick films. Such a

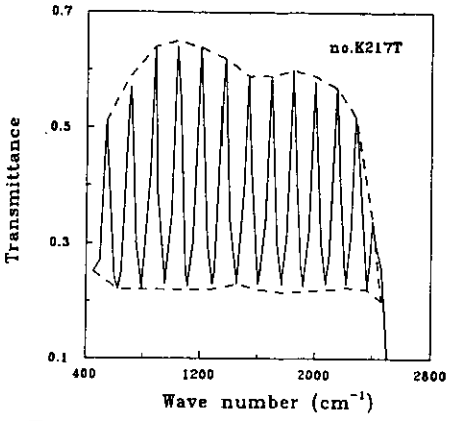

Figure 3. The transmittance interference spectrum of thick ($d = 5.6$ μm) sample KT217T.

modulated transmittance spectrum of a thick sample (sample K217T) is shown in figure 3.

We have investigated a large number of films, grown at various substrate temperatures (from room temperature to 300 °C), which hence have different contents of the HP phases in their strained sublayers.

3. Experiment and experimental results

The interference transmittance and reflectance spectra have been measured at room temperature in the range from 400 to 4000 cm^{-1} using a UR-20 double-beam spectrometer.

In the case of the thick films ($d > 2.5$ μm) the energy dependence of the refractive index $n(E)$ has been calculated from the minima and the maxima in the transmittance spectra. The energy dependence of the refractive index $n(E)$ in the case of the thin films was determined from the reflectance R and transmittance T spectra, by solving numerically the equations for the dependences of R and T on the real and imaginary parts of the refractive index, n and k, respectively, the wavelength of light, the film thickness d, the substrate thickness and the refractive index of the substrate, using the method described by Nilsson (1968).

The energy dependence of the refractive index $n(E)$ for samples with different thicknesses, containing all three PbTe crystal structure modifications are shown in figures 4 and 5. In the thicker films, shown in figure 4, the FCC phase prevails while, in the thinner films, the quantity of FCC phase is much smaller (figure 5). The $n(E)$ dependence of sample CR2K10T containing mainly BCC phase is given in figure 6. The same dependence for sample CR2K3T containing predominantly orthorhombic phase is given in figure 7. The reflectance electron microscopy studies indicate that the thickness of the upper FCC phase sublayer is of the order of the electron penetration depth (about 40 Å) in these samples as their electronograms show the presence not only of the FCC phase but also of the corresponding HP phases.

In both methods of calculation of $n(E)$ we have assumed a single-layer model which is sufficiently correct for the films consisting predominantly of one crystal phase.

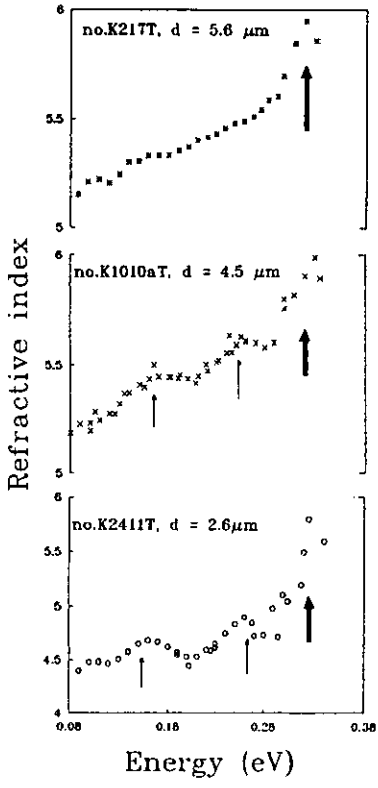

Figure 4. The dispersion of the refractive index in thick ($d = 2.5$–5.6 μm) samples. The bold arrows indicate the interband transition at 0.32 eV in the prevailing FCC phase. The thin arrows indicate the transitions across the junction; $E_p^{orth} - E_p^{FCC} = 0.15$ eV and 0.16 eV and $E_p^{FCC} - E_n^{orth} = 0.27$ eV and 0.26 eV for samples K2411T and K1010aT, respectively.

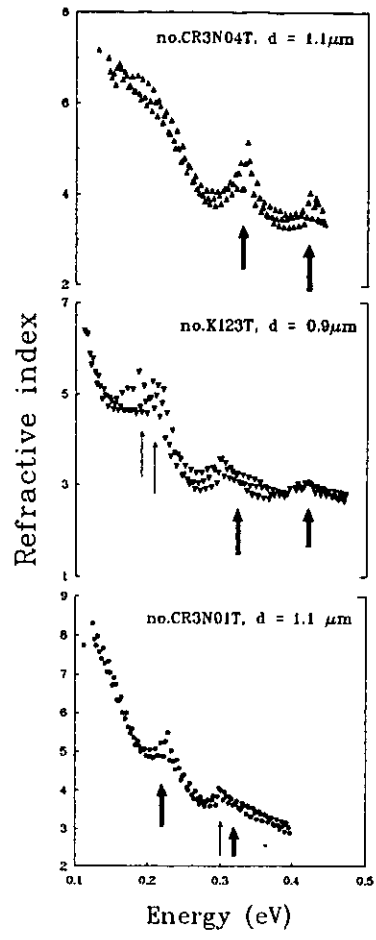

Figure 5. The dispersion of the refractive index in thin ($d \simeq 1$ μm) films. The bold arrows indicate the interband transitions: $E_g^{FCC} = 0.32$ eV and $E_g^{orth} = 0.42$ eV for samples CR3K04T and K123T; $E_g^{BCC} = 0.23$ eV and $E_g^{FCC} = 0.32$ eV for sample CR3K01T. The thin arrows indicate the transitions across the junction; $E_n^{BCC} - E_n^{orth} = 0.20$ eV and $E_p^{orth} - E_n^{BCC} = 0.22$ eV for sample K123T (see figure 11). The transition at 0.22 eV in this film screens the interband transition at 0.23 eV. The thin arrow at 0.30 eV for sample CR3K01T indicates the transition across the junction ($E_p^{BCC} - E_n^{FCC}$), screening the interband transition at 0.32 eV.

In the case of films with comparable quantities of two or three phases the refractive index energy dependence has to be considered in a qualitative way or, in other words, the behaviour of the refractive index in this sample is real, but its values are not.

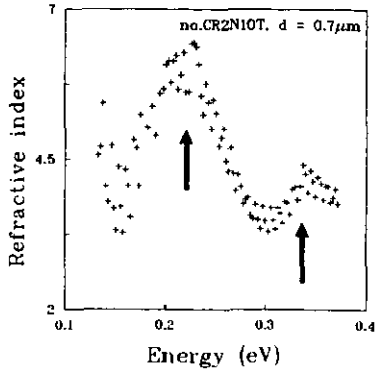

Figure 6. The dispersion of the refractive index of a sample containing solely BCC PbTe phase in the strained sublayer. The arrows indicate the interband transitions at 0.23 and 0.32 eV.

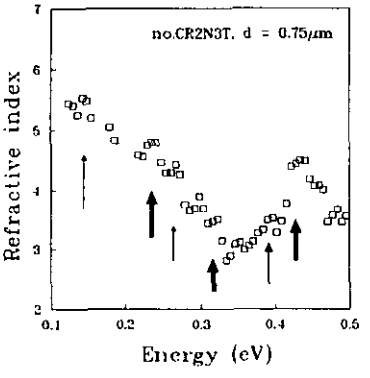

Figure 7. The dispersion of the refractive index of a sample with prevailing orthorhombic phase in the strained sublayer. The bold arrows indicate the interband transitions in all three phases: 0.23, 0.32 and 0.42 eV. The thin arrows correspond to the transitions across the junctions as follows: $E_p^{BCC} - E_n^{orth} = 0.39$ eV, $E_p^{orth} - E_n^{BCC} = 0.26$ eV and $E_n^{BCC} - E_n^{orth} = 0.16$ eV (see figure 11).

4. Discussion

It is well known that, in analysing the Kramers–Kronig relations, Velicky (1961) drew the conclusion that the maximum in the dispersion of the refractive index n corresponds to the strongest increase in the absorption coefficient. Thus the determination of the energy gap from the maximum in the energy dependence of the refractive index $n(E)$ is a common method. In the early investigations of Zemel *et al* (1965) the energy gap E_g of FCC PbTe at 300 K was determined to be 0.32 eV from the energy position of the maximum value of the refractive index, namely $n_\infty = 6.15$. Hence the maxima at 0.32 eV, which appear in our experimental $n(E)$ dependences correspond to the direct interband transitions at the L point of the Brillouin zone of FCC PbTe. The maximum value of the refractive index in the samples with significantly prevailing FCC phase (samples K217T, K1010aT and K2411T) is $n_\infty = 5.9$, in good

agreement with the results of Zemel *et al* (1965). The lower value of refractive index determined in our experiment may be accounted for by the presence of a strained sublayer, although the latter is comparatively much smaller than that of the basic film. The negligible thickness of the FCC phase sublayer in the films, in which the HP phases predominate leads to an unreal, much smaller value of n_∞ at 0.32 eV, but the peak still remains clearly resolved as the FCC structure always forms the upper sublayer.

4.1. Films containing BCC and FCC phases

The highest value of the refractive index in sample CR2K10T in which the BCC phase prevails, as seen from figure 6, is at 0.23 eV. The different crystal structure naturally implies a different electronic band structure and, in particular, a different energy gap. The more closely packed crystal structure (as the BCC PbTe appears to be, compared with the FCC PbTe), in general, leads to a smaller energy gap. Then one may assume a smaller energy gap E_g in the HP BCC phase, which has a smaller lattice constant. So it is quite reasonable to assign the peak in the dispersion of the refractive index at 0.23 eV to direct interband transitions in the BCC PbTe. As theoretical calculations of the BCC PbTe energy band structure are not available, we are not able to decide at which symmetry point of the Brillouin zone these transitions take place, but this certainly is not the point with L symmetry (as in FCC PbTe), as there is no point with such symmetry in the BCC crystal structure. The higher value of the refractive index $n_\infty = 6.5$ in BCC PbTe compared with FCC PbTe corresponds to its smaller energy gap. It is worth mentioning that the values of the BCC PbTe energy gap and n_∞ determined in these experiments coincide with the values obtained for very thin films (about 100 nm) (Baleva 1986), where the determination of the optical constants is highly complicated.

Although the quantity of FCC phase in this group of films is negligible (the thickness of the upper sublayer is about 40 Å), a maximum in the $n(E)$ dependence at 0.32 eV is still clearly resolved. Then the energy profile of sample CR2K10T is as shown in figure 8. In the figure, E_p^{BCC} and E_n^{BCC} are the energies of the valence band (VB) top and the conduction band (CB) bottom for the BCC phase PbTe, and E_p^{FCC} and E_n^{FCC} are the corresponding values for the FCC phase. This energy profile is in fact a heterophase junction, whose thickness has to be comparatively small as it follows from the sharp phase transition from BCC to FCC phase (see figure 2). In such a structure, apart from the interband transitions, transitions across the junction ($E_p^{BCC} \rightarrow E_n^{FCC}$, $E_p^{FCC} \rightarrow E_p^{BCC}$, $E_n^{BCC} \rightarrow E_n^{FCC}$ and $E_p^{FCC} \rightarrow E_n^{BCC}$) have to take place as well. The energy of each of the transitions $E_p^{FCC} \rightarrow E_p^{BCC}$ and $E_n^{BCC} \rightarrow E_n^{FCC}$ can vary from 0 to 0.09 eV, and the energy of the transitions $E_p^{BCC} \rightarrow E_n^{FCC}$ and $E_p^{FCC} \rightarrow E_n^{BCC}$ from 0.23 to 0.32 eV. In sample CR2K10T (figure 6) the energy of the transition $E_p^{BCC} \rightarrow E_n^{FCC}$ (or $E_p^{FCC} \rightarrow E_n^{BCC}$) is obviously 0.32 eV and that of $E_n^{BCC} \rightarrow E_n^{FCC}$ (or $E_p^{FCC} \rightarrow E_p^{BCC}$) is 0.09 eV; this is confirmed by the increase in $n(E)$ at energies below 0.15 eV. The increase in the thickness of the upper FCC sublayer, in general, must affect the Fermi level position and hence must change the heterophase junction transition energies. The latter is demonstrated by the $n(E)$ behaviour of sample CR3K01T, shown in figure 5, grown at $T_s = 50\,^{\circ}C$ and thus containing BCC and FCC phases. In this sample the energy of the transition $E_p^{BCC} \rightarrow E_n^{FCC}$ (or $E_p^{FCC} \rightarrow E_n^{BCC}$) is most probably 0.30 eV. The energy value of

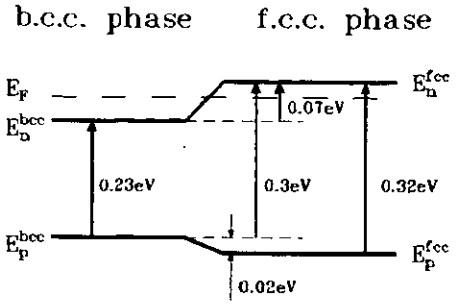

Figure 8. Schematic diagram of the energy profile of films containing entirely BCC phase in the strained sublayer.

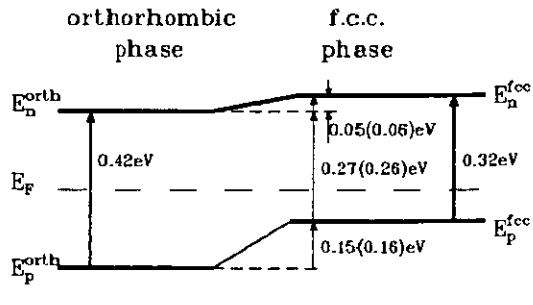

Figure 9. Schematic diagram of the energy profile of films with orthorhombic phase predominating in the strained sublayer and a sufficiently thick upper FCC sublayer.

0.30 eV is very close to the FCC phase energy gap (0.32 eV); so the heterophase transition and the FCC phase interband transitions can hardly be detected separately.

To summarize, the energy profiles of the films grown at $T_s \leqslant 50\,°C$ are as shown in figure 8. In this figure the positions of the energy levels hold for sample CR3K01T.

4.2. Films with BCC and orthorhombic phases in the strained sublayer

The energy dependence of the refractive index of a film with prevailing orthorhombic phase in the strained sublayer (sample CR2K3T) is given in figure 7. A clearly defined peak can be seen at 0.42 eV, where the value of the refractive index is $n_\infty = 4.5$. The peaks that correspond to the interband transitions in the BCC and FCC phases are present as well, although they are not so clearly resolved. The comparatively high value of the refractive index at energies lower than 0.32 eV indicates some additional transitions. If we take into account that in this film the BCC and FCC PbTe phases are present in comparable quantities and that the BCC and orthorhombic phases are mixed in the strained sublayer, the identification of the additional transitions is ambiguous.

Identification of the transitions between the orthorhombic and the FCC phases becomes possible in films with a thick upper sublayer (containing FCC phase).

Then the films with BCC and orthorhombic phases in the strained sublayer can be divided into two groups as follows.

4.2.1. Samples with orthorhombic phase predominating in the strained sublayer and thick FCC phase upper sublayer. We succeeded in identifying two of the interphase transitions in the films where the orthorhombic phase prevails in the strained sublayer and the upper FCC phase sublayer is sufficiently thick (figure 4, samples K2411T and K1010aT). In the dispersion of the refractive index of the thickest sample K217T, only one peak is seen at 0.32 eV. On decrease in the film thickness, i.e. on decrease in the quantity of the FCC phase, two lower-energy peaks appear at 0.16 and 0.26 eV for sample K1010aT and at 0.15 and 0.27 eV for sample K2411T. The resolution of these peaks increases with decrease in the quantity of FCC phase. Taking all this into account, we related the peak at 0.42 eV to the direct energy gap of orthorhombic PbTe and the additional peaks to transitions across the potential barrier formed in the heterophase junction between the orthorhombic and FCC phases. The energy profiles of this structure for samples K2411T and K1010aT are shown in figure 9 (the energies

of the transitions for sample K1010aT are given in parentheses). In this figure, E_p^{orth} and E_n^{orth} are the energies of the VB top and the CB bottom of the orthorhombic phase PbTe. The transitions at the BCC and orthorhombic phase boundaries can be neglected in the case of thicker films, as the quantity of BCC is negligible compared with the remaining two phases in figure 9. The maxima at 0.15 and 0.16 eV can be attributed to the transition $E_p^{orth} \rightarrow E_p^{FCC}$, and those at 0.27 and 0.26 eV to the transition $E_p^{FCC} \rightarrow E_n^{orth}$. The fact that the energies of these transitions vary from sample to sample confirms the assumption that they are not interband transitions in one and the same phase. The energies of the junction transitions are those which vary with the Fermi level position, which is different in different films. The estimated values of the junction transitions again give a value of 0.42 eV for the energy gap of the orthorhombic PbTe phase.

Such an energy profile must influence the temperature dependence of the Hall coefficient R_H and the electrical conductivity σ. The activation energy of 0.05 (0.06) eV, which follows from figure 9, has to govern the temperature dependence of the Hall mobility $\mu(T) = \sigma(T)R_H(T)$. In figure 10 the $\mu(T)$ dependences of samples K217T, K2411T and K1010aT are shown. The $\mu(T)$ dependence of sample K217T does not vary from that typical for the bulk FCC PbTe, as the quantity of HP phases in this film is negligible ($d = 5.6$ μm). The same dependence of sample K2411T indicates the presence of a potential barrier with an energy $\Delta E = 0.047$ eV, which is exactly the energy difference $E_n^{FCC} - E_n^{orth}$ (figure 9). The same holds for the $\mu(T)$ dependence of sample K1010aT, but the energy difference $\Delta E = E_n^{FCC} - E_n^{orth}$ in this case is determined to be 0.06 eV. Thus the electrical measurements verify the correctness of the assumed energy profile.

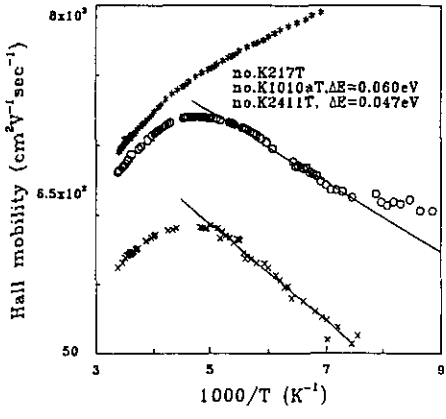

Figure 10. The temperature dependence of the Hall mobility in thick samples. Here $\Delta E = E_n^{FCC} - E_n^{orth}$.

The orthorhombic PbTe phase is intermediate between the FCC and the BCC phases; so it is reasonable to expect an intermediate value of the energy gap E_g, but our experiment gives the highest value of E_g for this phase. This can be easily understood if we bear in mind that the lowest-energy interband transitions in the orthorhombic structures were determined to be either direct forbidden or indirect (Lukes *et al* 1988). We believe that the additional low-energy peaks observed in the

dispersion of the refractive index of our samples with orthorhombic phase are not of this nature, as the absorption coefficient in the case of indirect or direct forbidden transitions is small and probably will not cause any apparent peculiarities. Apart from this, as has already been pointed out, the energy of these maxima changes from one sample to another, which is possible only if they are junction transitions.

Thus the energy profile of the films grown at $T_s \geqslant 200\,°C$ and with comparatively thick FCC phase upper sublayer are as schematically presented in figure 9.

4.2.2. Films containing comparable quantities of all three phases with a thin upper FCC phase sublayer. In the energy dependence of the refractive index $n(E)$ of sample CR2K3T the contribution of the transitions between the mixed orthorhombic and BCC phase in the dispersion of the refractive index has to be greater than that of the transitions across the heterophase junctions, on account of the negligible quantity of FCC phase. The same situation must occur in samples containing comparable quantities of all three phases grown at $T_s \simeq 100\,°C$. The energy profile of such structures is shown in figure 11. The behaviour of the $n(E)$ dependence of sample CR2K3T (figure 7) and sample K123T (figure 5) corresponds to the transition energies shown in figure 11 (the values in parentheses are for sample K123T).

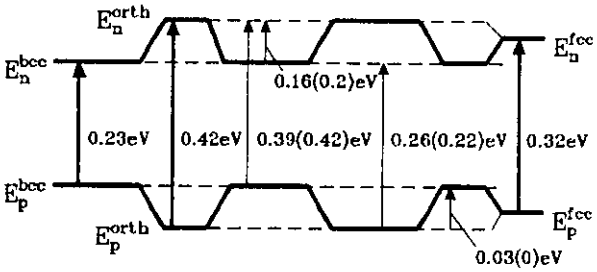

Figure 11. Schematic diagram of the energy profile of films containing comparable quantities of all three phases.

Thus, in the samples grown at $T_s \simeq 100\,°C$, when the quantity of FCC phase is small (films with thickness of about 1 μm), the absorption is due mainly to the transitions across the potential barrier formed at the boundaries of the grains with different HP phases. As seen from figure 11, except for the identified transitions between the mixed HP phases, transitions between the BCC and the FCC phases and between the orthorhombic and the FCC phases can take place as well. It is complicated to identify each of the large variety of transitions without knowing the position of the Fermi level in the different phases. The strong increase in the refractive index at energies lower than 0.20 eV in samples CR2K3T, CR3K04T and K123T indicates the presence of transitions with close transition energies.

5. Conclusion

On the grounds of the experimental study of the transmittance and the reflectance of polymorphous PbTe and PbTe:Cr films on KCl substrates we have succeeded in determining the energy gaps of the BCC PbTe ($E_g = 0.23$ eV) and orthorhombic

PbTe (E_g = 0.42 eV) crystal phases; this to our knowledge has not previously been achieved.

These investigations, together with the crystal structure studies, demonstrate that the films under consideration are in fact a new type of semiconductor junction, which can be called a heterophase junction. Such structures can be formed, obviously, using highly non-equilibrium techniques of growth, one of which is LAD. PbTe, which crystallizes in three different pressure-dependent modifications, offers the possibility of fabricating two different kinds of heterophase junction by varying the technological conditions.

Acknowledgments

The work has been financially supported by the Ministry of Education and Science under contract Φ–47.

References

Baleva M 1986 *Thin Solid Films* **139** L71
Baleva M, Bozukov L and Momtchilova M 1992a *J. Phys.: Condens. Matter* **4** 4633
Baleva M, Ivanov I and Momtchilova M 1992b *J. Phys.: Condens. Matter* **4** 4645
Chattopadhyay T, Werner A and von Schnering H 1984 *High Pressure in Science and Technology (Mater. Russ. Soc. Symp. Proc. 22)* ed C G Human, R K MacCrane and E Whalley (New York: Elsevier) p 93
Fujii Y, Kitamura K, Onodera A and Yamada Y 1984 *Solid State Commun.* **49** 135
Lukes F and Dub P 1988 *Optical Properties of GeS, GeSe, SnS and SnSe* (Brue: Univerzita)
Nilsson P O 1968 *Appl. Opt.* **7** 435
Velicky B 1961 *Czech. J. Phys.* B **11** 541
Wakabayashi I, Kobayashi H, Nacasaki H and Minomura S 1968 *J. Phys. Soc. Japan* **1** 227
Zemel J N, Jensen J D and Schoolar R B 1965 *Phys. Rev.* **140** A330